Supplementary Information

A Dual-Functional Surfactant Strategy for In-Situ Sulfur Doping and Pore Engineering of Cyclodextrin-Derived Carbon Microspheres toward Supercapacitor and Desalination Applications

Shuaiqi Liu, Yiduo Liu, Yinglong Xu, Zeming Liu, Jingjing Hao, Xiaohui Huang and Qinghan Meng*

Experimental Section

Materials

β-Cyclodextrin was supplied by Tianjin Huasheng Chemical Reagents. Sodium lignosulfonate (NaLS) was provided by Shanghai Yuanye. Pluronic F127 triblock copolymer ($PEO_{106}PPO_{70}$-PEO_{106}, Mw ~13000) was supplied by Shanghai McLean. Acetylene black and polytetrafluoroethylene (PTFE) were both provided by Shanghai Aladdin. Potassium hydroxide (KOH) was supplied by Fuchen Chemical.

Structural Characterization

The surface morphology of the material was observed using a scanning electron microscope (SEM) equipped with the German ZEISS Sigma 360 system. The Fourier transform infrared spectroscopy was performed using a Nicolet 8700 FTIR spectrometer. The pyrolytic behaviour of the precursor was studied using a Mettler Toledo TGA/DSC1 thermogravimetric analyser (heating rate: 10 ℃ min^{-1}). XRD measurements were conducted with an Ultima IV instrument employing Cu-targeted Kα radiation. Raman spectroscopy was performed using a HORIBA XploRA PLUS Raman spectrometer equipped with a 532 nm incident laser. The nitrogen (N_2) adsorption-desorption isotherm was measured using a Quantachrome Autosorb-1 (USA). The specific surface area was measured using the Brunner-Emmett-Teller (BET) method, while the total pore size distribution was obtained through DFT modelling and the micropore size distribution was determined by the HK method. The surface chemical composition of spherical activated carbon was characterised using X-ray photoelectron spectroscopy (XPS) (Thermo Scientific K-Alpha, USA). Water contact angle measurements were performed using a Dataphysics OCA20 water contact angle measuring instrument.

Electrochemical Characterization

The active material, acetyleneblack, and polytetrafluoroethylene should be mixed in a mass ratio of 8:1:1. The utilisation of anhydrous ethanol as the dispersant is imperative for the successful blending of the mixture in a mortar, ensuring its uniformity. The mixture should then be applied to an 11 mm diameter foam nickel disc, which will act as the current collector, thus yielding the desired electrode material.

Cyclic voltammetry (CV) was performed using 6 M KOH as the electrolyte within a potential window of -1 to 0 V. The reference electrode was supplied by Lerton and was an Hg/HgO electrode. The counter electrode was a platinum electrode and the working electrode was a nickel electrode that had been prepared for use. The three electrodes formed a three-electrode system for testing.

The formula for quantitatively calculating the specific capacitance using the obtained CV curve is as follows:

$$C_s = \frac{\int IdV}{2mv\Delta V} \qquad \text{* MERGEFORMAT (S1)}$$

Here, C_s represents the specific capacitance of the electrode material, m denotes the mass of active material contained on the electrode plate as determined by weighing, v indicates the scanning rate of the applied voltage, and ΔV signifies the applied potential window (set to -1 to 0 V in this experiment). The integral ∫ IdV in the equation represents the integration of the current I over the voltage V.

Prior to testing, electrode sheets must be soaked in 6 M KOH solution for 30 minutes. To investigate the capacitive properties, reversibility, and rate performance of the material, a scanning rate gradient was set during testing. The scanning rates were set to 1 mV s^{-1}, 2 mV s^{-1}, 5 mV s^{-1}, 10 mV s^{-1}, and 20 mV s^{-1}. The material was studied based on the shape and area of the cyclic voltammetry curves.

To investigate the capacitive contribution rate of the material, the current density i(V) at a fixed potential is divided into two components: (a) the current density $k_2v^{1/2}$ associated with diffusion-controlled redox processes; and (b) the current density k_1v associated with surface-controlled processes. The capacitive contribution is calculated using Equation S2.

$$i(V) = k_1 v + k_2 v^{1/2} \qquad \text{* MERGEFORMAT (S2)}$$

The voltage window for constant current discharge (GCD) testing spans 0-1 V. By controlling a specific current density, the time required for voltage changes is recorded to generate a voltage-time curve. The material's performance is then qualitatively or quantitatively assessed based on the curve's shape and charge/discharge duration. The formula for quantitatively calculating specific capacitance using this curve is as follows:

$$C_s = \frac{2It}{m\Delta V} \qquad \text{* MERGEFORMAT (S3)}$$

C_s represents the specific capacitance of the electrode material, m denotes the mass of active material on the electrode plate as determined by weighing, I indicates the magnitude of current applied to the electrode, t signifies the duration of charging or discharging (in this experiment, discharge time is used to calculate specific capacitance), and ΔV represents the potential window.

Electrochemical impedance spectroscopy (EIS) was used to measure the resistance of these electrode materials during electrochemical processes. The test frequency range was 10 mHz to 100 kHz, with an amplitude of 5 mV. Signals within this range were applied to the materials, ultimately yielding EIS curves. The EIS measurement system was identical to that used for CV measurements and comprised a three-electrode system containing three electrodes and an electrolyte.

Capacitive deionization (CDI) testing

The CDI electrode was prepared by mixing the active material with acetylene black and polytetrafluoroethylene at a weight ratio of 8:1:1. The resulting mixture was coated onto a foam nickel plate measuring 5 cm × 6 cm and dried at 70 ℃ for 12 hours. Tableting was performed using a powder tablet press at 10 MPa for 30 seconds. The mass of the active material was determined by weighing the plate before and after coating.

Testing was conducted with applied voltages ranging from 1.0 V to 1.4 V, sodium chloride solution concentrations between 100 and 1600 mg L^{-1}, and flow rates ranging from 10 to 40 mL min^{-1}. The test temperature for capacitive deionisation experiments was maintained at 25 ℃.

The formula for calculating the electrosorption capacity is as follows:

$$q_e = \frac{(C_0 - C_e)V}{m} \qquad \text{* MERGEFORMAT (S4)}$$

C_0 and C_e denote the initial concentration and equilibrium concentration of the salt solution, respectively, in units of mg mL^{-1}. V represents the volume of the salt solution, which is 200 mL. m denotes the mass of the active material on both electrode plates.

The formula for ion removal rate is as follows:

$$S = \frac{Q}{t} \qquad \text{* MERGEFORMAT (S5)}$$

S denotes the ion removal rate, expressed in mg g^{-1} s^{-1}. Q denotes the electrosorption capacity. t denotes time, expressed in seconds.

$$q_e = \frac{q_m K_L C_e}{1 + K_L C_e} \qquad \text{* MERGEFORMAT (S6)}$$

The Langmuir isotherm equation (Formula S6) is one of the fitting methods commonly used to determine whether a material exhibits monolayer adsorption. Here, q_e represents the equilibrium electrosorption capacity per unit mass, q_m denotes the maximum theoretical adsorption capacity per unit mass (under monolayer adsorption conditions), C_e is the equilibrium concentration, and K_L is the Langmuir constant.

$$q_e = K_F C_e^{1/n} \qquad \text{* MERGEFORMAT (S7)}$$

The Freundlich isotherm equation (Formula S7) is another commonly used fitting method, typically employed to determine whether a material exhibits multi-layer adsorption. Here, q_e represents the equilibrium electrosorption capacity per unit mass, C_e denotes the equilibrium concentration, while n and K_F are constants. Specifically, n is the adsorption index and K_F is the Freundlich constant.

Other formulas used are as follows:

$$d = n\lambda / 2\sin(\theta) \qquad \text{* MERGEFORMAT (S8)}$$

Formula S8 represents Bragg's Law, where d denotes the interplanar spacing, θ is the angle between the incident X-rays and the corresponding crystal plane, and λ is the wavelength of the X-rays.

$$L_a = \frac{1.84\lambda}{B_{100}\cos\theta_{100}} \quad \text{* MERGEFORMAT (S9)}$$

Formula S9 represents the Scherrer equation, where λ denotes the X-ray wavelength (0.154178 nm), B_{100} is the full width at half maximum of the (100) peak, and $2\theta_{100}$ is the corresponding peak position.

Table S1. Comparison of Parameters for Different Reaction Conditions (Other Conditions Held Constant)

Sample Name	Preheating Temperature (℃)	Carbonization Temperature (℃)	NaLS (g)
ACCM-0	Pre-oxidation 300	800	0.00
ACCM-1	Pre-oxidation 300	800	0.05
ACCM-2	Pre-oxidation 300	800	0.10
ACCM-3	Pre-oxidation 300	800	0.20
ACCM-4	Pre-oxidation 250	800	0.10
ACCM-5	Pre-oxidation 350	800	0.10
ACCM-6	Pre-carbonization 300	700	0.10
ACCM-7	Pre-carbonization 300	800	0.10
ACCM-8	Pre-carbonization 300	900	0.10

Table S2. XPS Elemental Composition of ACCMs with Different Sodium Lignosulfonate Contents

Sample Name	C (%)	O (%)	S (%)
ACCM-0	90.83	9.17	
ACCM-1	87.55	12.26	0.19
ACCM-2	83.66	16.10	0.24
ACCM-3	82.22	17.27	0.52

Table S3. BET Data for ACCMs with Different Sodium Lignosulfonate Contents

Sample Name	S_{BET} ($m^2 g^{-1}$)	Average pore size (nm)	Total pore volume ($cm^3 g^{-1}$)	Micropore volume ($cm^3 g^{-1}$)	Micropore area ($m^2 g^{-1}$)
ACCM-0	101.54	3.75	0.10	0.01	13.40
ACCM-1	545.02	1.73	0.24	0.22	534.54
ACCM-2	828.67	1.54	0.32	0.32	826.02
ACCM-3	1066.50	1.57	0.42	0.41	1050.00

Table S4. Specific parameters for fitting the electroadsorption data of ACCM-2 using the Langmuir and Freundlich models

Isotherm model	Correlation parameter	ACCM-2
Langmuir	q_m	86.80556
	K_L	0.000565
	R^2	0.98215
Freundlich	K_F	0.052068
	n	1.042188
	R^2	0.98546

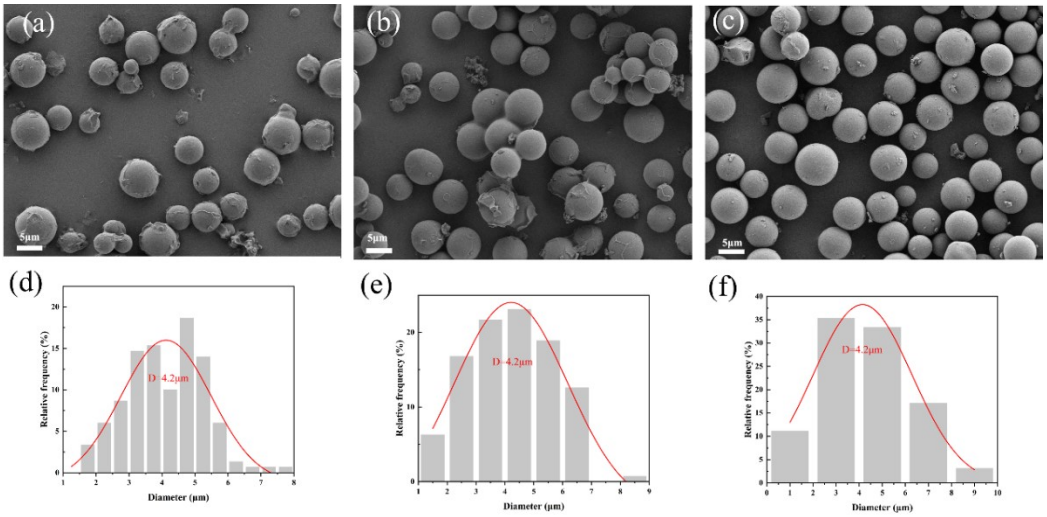

Figure S1. (a) to (c) show SEM images of HCCMs at different hydrothermal times (6, 9, 12 h), while (d) and (e) present the corresponding particle size distribution curves for (a) to (c), respectively.

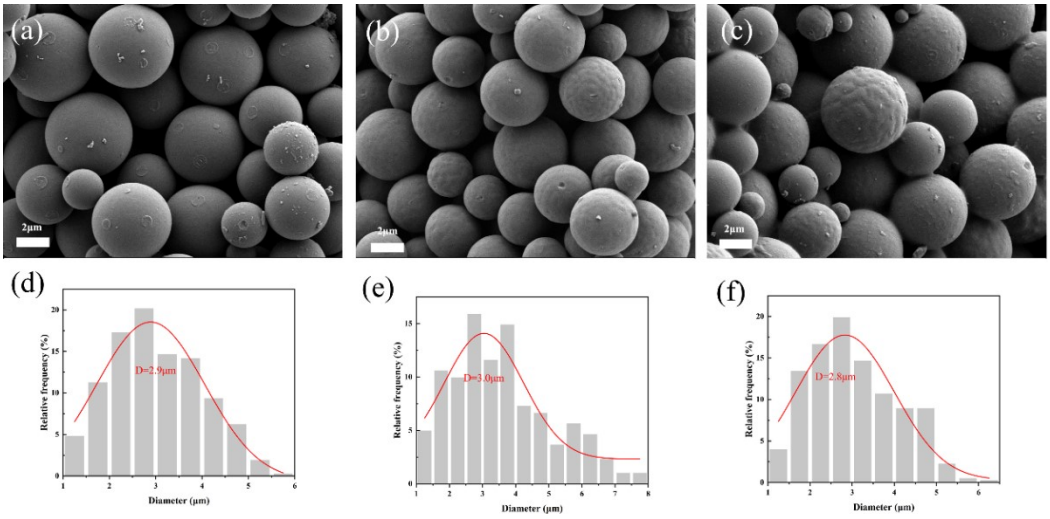

Figure S2. (a) to (c) show SEM images of ACCMs at different pre-oxidation temperatures (250 ℃, 300 ℃, 350 ℃), while (d) to (f) present their corresponding particle size distribution curves.

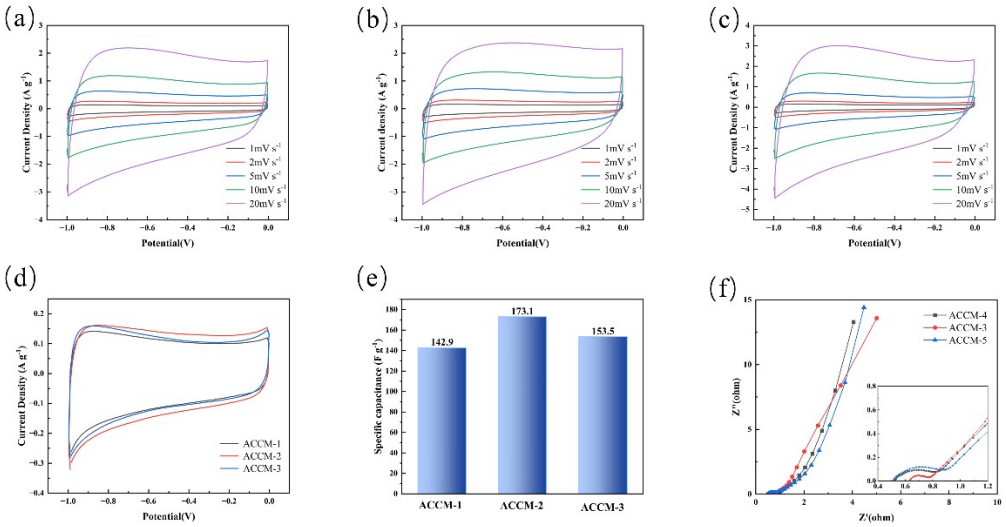

Figure S3. (a) to (c) show the CV curves of ACCMs at different pre-oxidation temperatures (250 ℃, 300 ℃, 350 ℃) under scan rates of 1–20 mV s^{-1}, (d) CV curves of the three spherical activated carbon samples at a scan rate of 1 mV s^{-1}. (e) Specific capacitance of the three spherical activated carbon samples at a scan rate of 1 mV s^{-1}. (f) EIS plots of the three spherical activated carbon samples, with insets showing enlarged views.

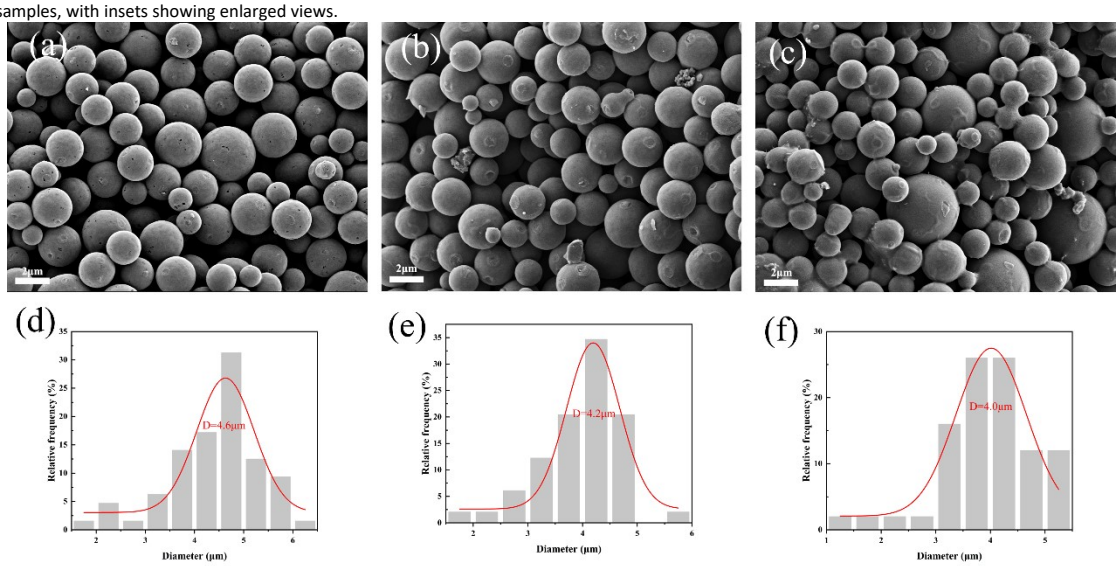

Figure S4. (a) to (c) show SEM images of ACCMs at different carbonization temperatures (700 ℃, 800 ℃, 900 ℃), while (d) to (f) present their corresponding particle size distribution curves.

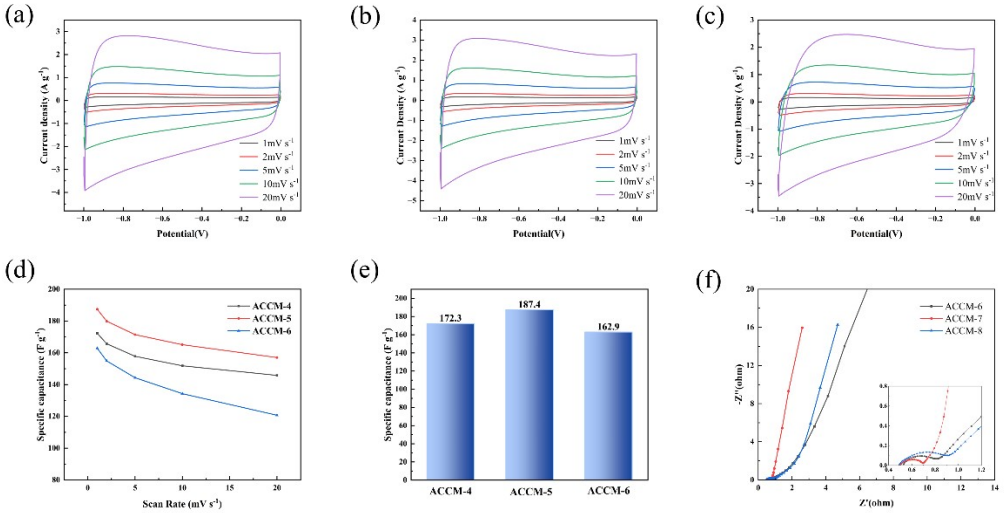

Figure S5. (a) to (c) show the CV curves of ACCMs at different carbonization temperatures (700 ℃, 800 ℃, 900 ℃) under scan rates of 1–20 mV s^{-1}, (d) CV curves of the three spherical activated carbon groups at a scan rate of 1 mV s^{-1}; (e) Specific capacitance of the three spherical activated carbon groups at a scan rate of 1 mV s^{-1}; (f) EIS plots of the three spherical activated carbon samples, with insets showing enlarged views.

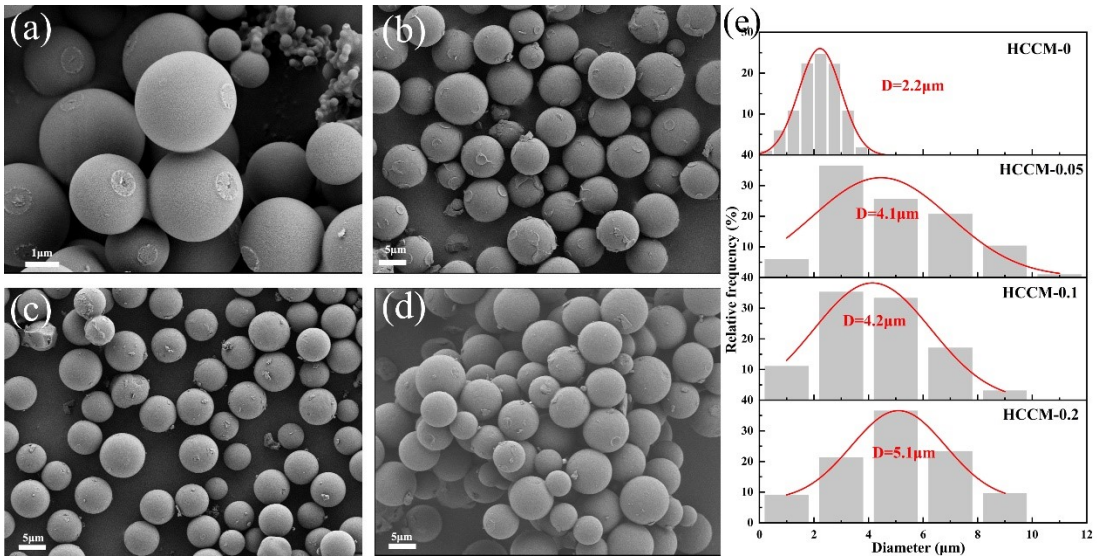

111
112 **Figure S6.** (a) to (d) show SEM images of HCCMs with different sodium lignosulfonate contents (0, 0.05, 0.1, 0.2 g). (e) presents the particle size distribution corresponding to (a) to (d).

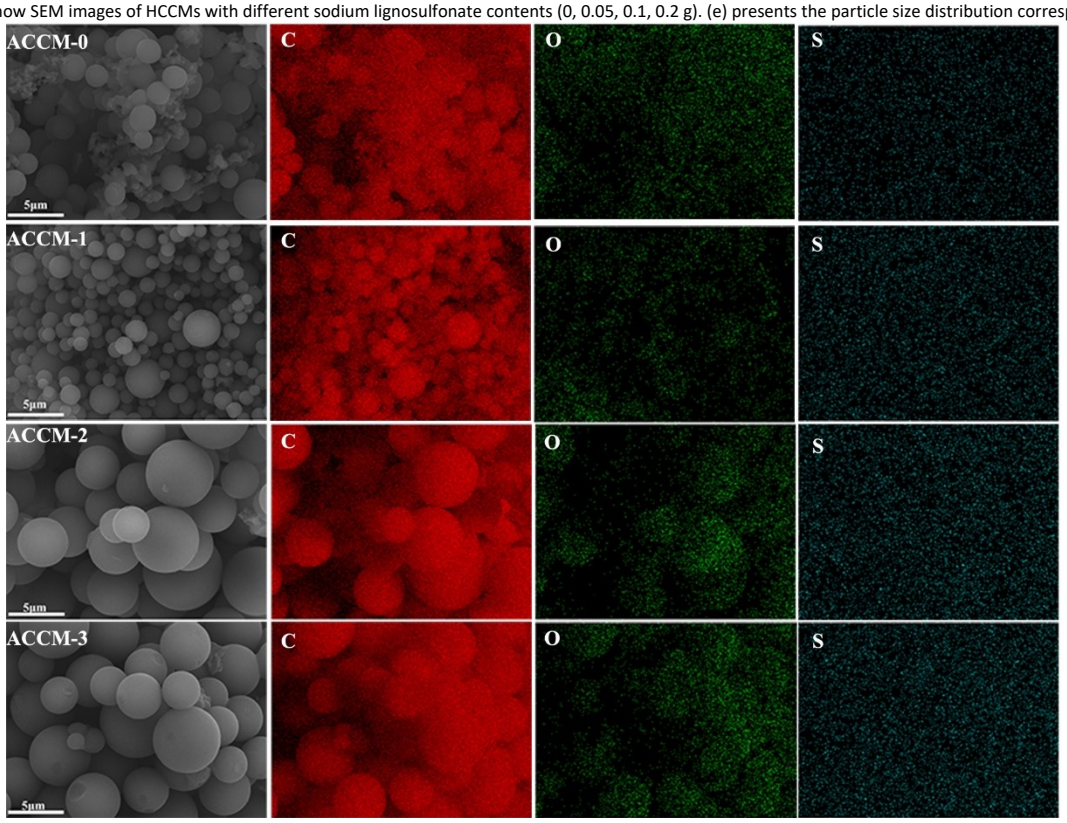

113
114 **Figure S7.** EDS elemental distribution maps of ACCMs with different sodium lignosulfonate contents

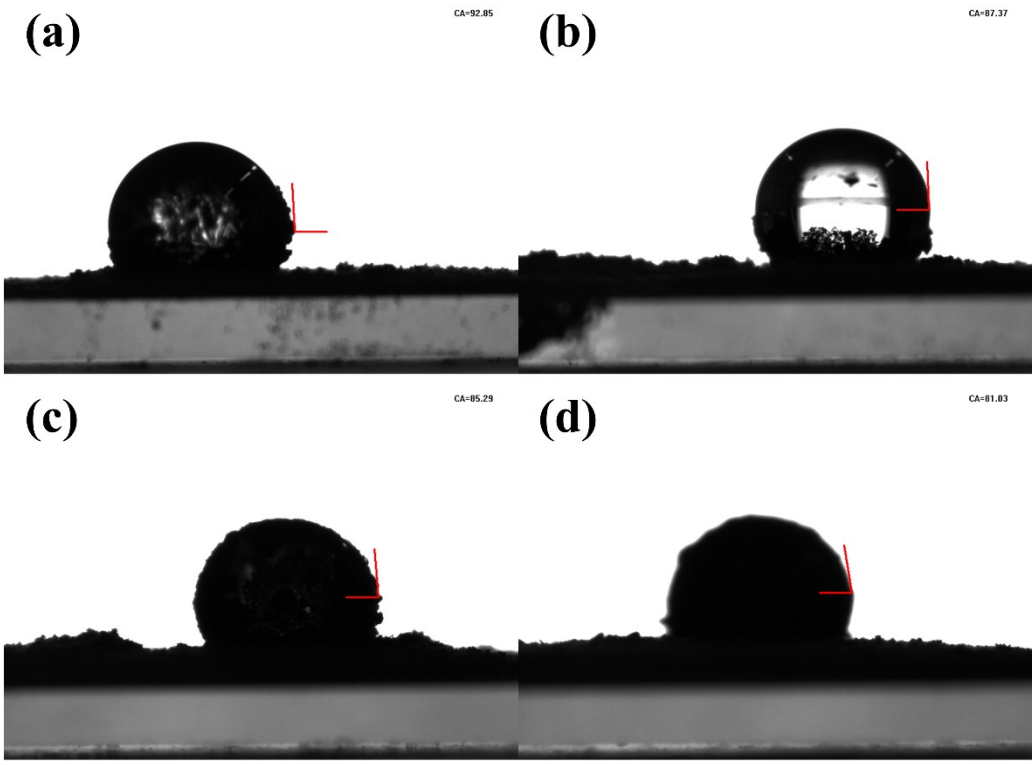

Figure S8 Images of water contact angles for (a) ACCM-0, (b) ACCM-1, (c) ACCM-2, and (d) ACCM-3

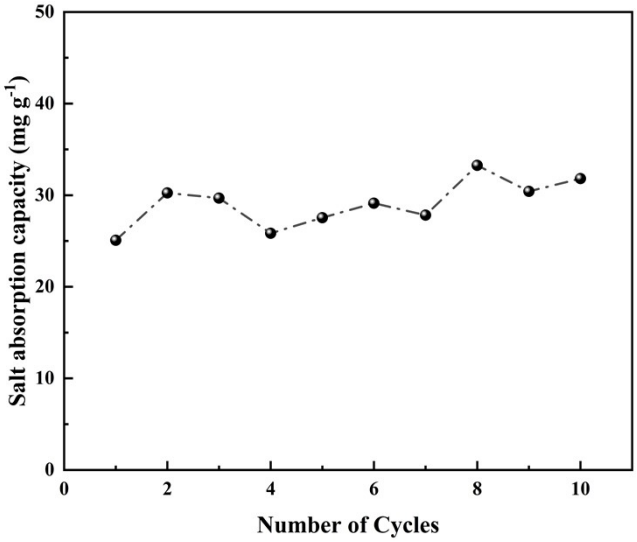

Figure S9. Electroadsorption desalination capacity of ACCM-2 at the tenth equilibrium.

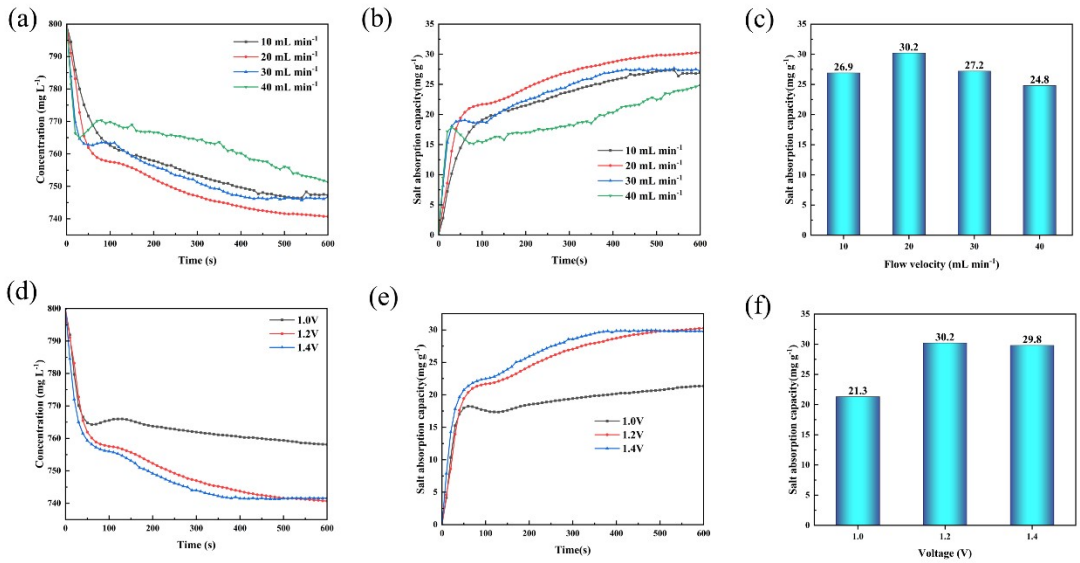

Figure S10. At different test flow rates: (a) salt concentration variation over time, (b) electroadsorption desalination rate variation over time, (c) electroadsorption desalination rate at various test flow rates. At different applied voltages: (d) salt concentration variation over time, (e) electroadsorption desalination rate variation over time, (f) electroadsorption desalination rate at various applied voltages.

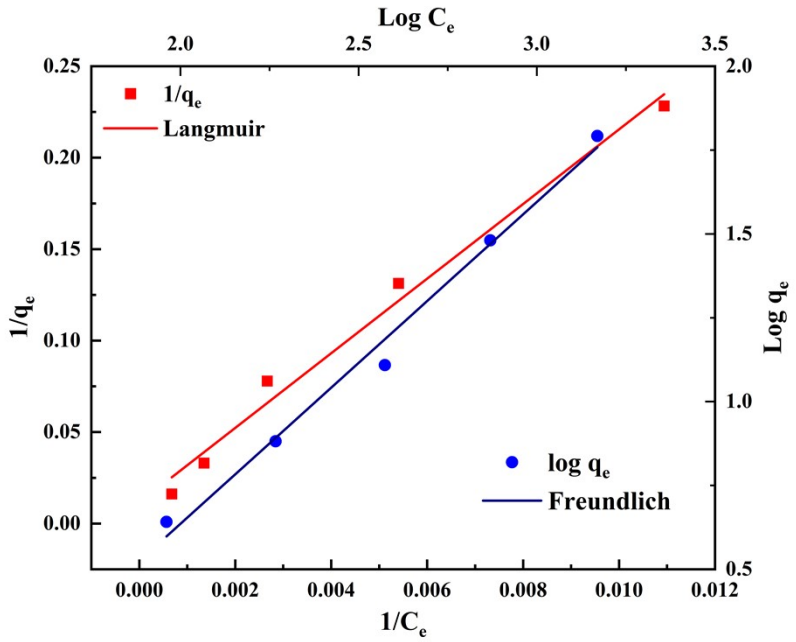

Figure S11. Fitted images of Langmuir and Freundlich adsorption isotherms for ACCM-2

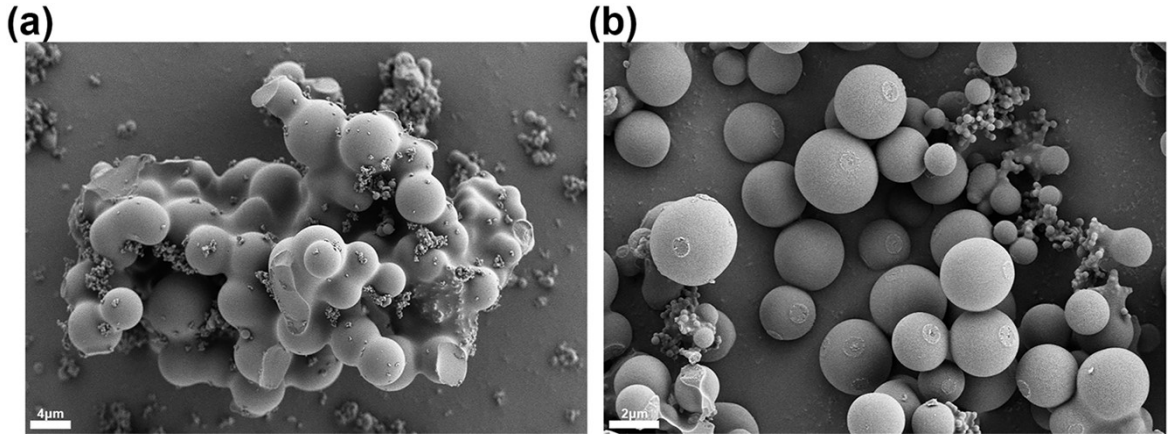

Figure S12: Using 5g β-cyclodextrin as the raw material and 60 ml deionized water as the solvent, a hydrothermal reaction was conducted at a hydrothermal temperature of 200℃ and a hydrothermal time of 12 hours. (a) shows the SEM image obtained without adding Pluronic F127 during the hydrothermal process; (b) shows the SEM image obtained after adding 0.125 g Pluronic F127 under the same conditions during the hydrothermal process.

As shown in Figure S12, the spherical aggregates prepared by hydrothermal method using only β-cyclodextrin as the raw material were severely aggregated, and there were a large number of small-diameter aggregated structures around them. After adding Pluronic F127, the spherical aggregates significantly decreased, but two different-sized spherical structures still appeared. By taking advantage of the high molecular weight and the charge of lignosulfonate sodium, the water heating process to some extent inhibited the nucleation of small spheres and reduced the aggregated structures of small diameters, thereby improving the spherical morphology.

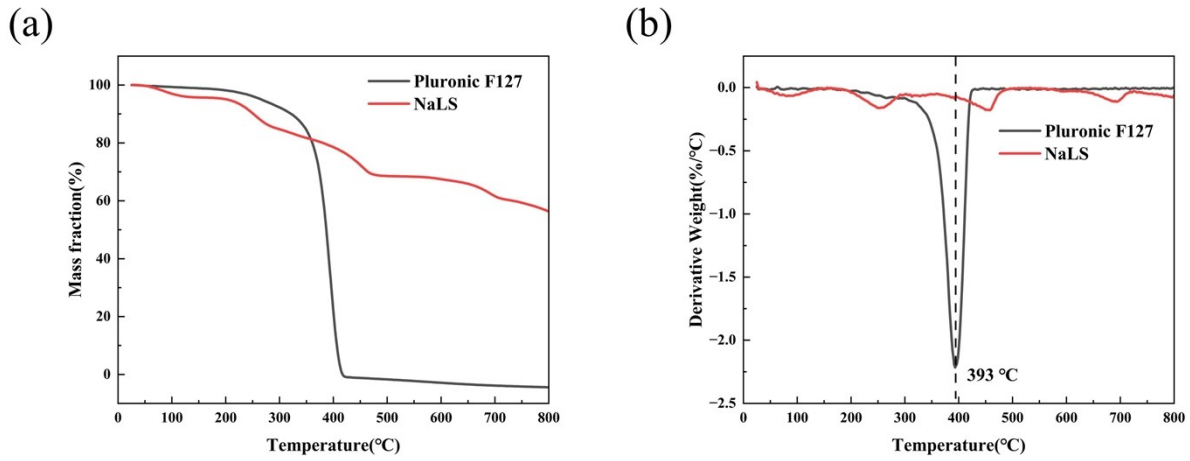

Figure S13 Thermal degradation and differential thermal degradation curves of Pluronic F127 and NaLS

The results show that Pluronic F127 exhibits a significant weight loss peak near 400 ℃, and the yield approaches zero after 400 ℃; while NaLS has two weak weight loss peaks after 400 ℃, with the weight loss peak around 455 ℃ corresponding to the intense thermal decomposition of the aromatic framework, and the weight loss peak around 688 ℃ attributed to the further condensation of the coke formed in the earlier stage of thermal decomposition or the decomposition of inorganic salts. During the carbonization process, when the temperature rises to 400 ℃, the aromatic carbon fragments formed by NaLS may deposit in the mesopores formed by the thermal decomposition of F127, thereby further increasing the proportion of micropores.